

# Deposition of Graphene and related nanomaterials by dynamic spray-gun method: a new route to implement nanomaterials in real applications

## Authors

**Paolo Bondavalli**

*Laboratoire de Chimie et des Matériaux Multifonctionnels, Thales Research and Technology, 1 Av. A. Fresnel, 91767 Palaiseau, France*

**Didier Pribat**

*Laboratoire de Physique des Couches Minces, Ecole Polytechnique, 1 Av. A. Fresnel, 91767 Palaiseau, France*

**Pierre Legagneux**

*Laboratoire Micro Nano Systèmes, Thales Research and Technology, 1 Av. A. Fresnel, 91767 Palaiseau, France*

**Marie-Blandine Martin**

*Laboratoire des Technologies Avancées, Thales Research and Technology, 1 Av. A. Fresnel, 91767 Palaiseau, France*

**Louiza Hamidouche**

*Laboratoire Micro Nano Systèmes, Thales Research and Technology, 1 Av. A. Fresnel, 91767 Palaiseau, France*

**Lilia Qassym**

*Laboratoire de Chimie et des Matériaux Multifonctionnels, Thales Research and Technology, 1 Av. A. Fresnel, 91767 Palaiseau, France*

**Aikaterini Flora Trompeta**

*Research Unit of Advanced, Composite, Nanomaterials and Nanotechnology, School of Chemical Engineering, National Technical University of Athens, 9 Heroon Polytechniou st., Zografos, Athens, GR-15773*

**Costantinos Charitidis**

*Research Unit of Advanced, Composite, Nanomaterials and Nanotechnology, School of Chemical Engineering, National Technical University of Athens, 9 Heroon Polytechniou st., Zografos, Athens, GR-15773*

## Abstract

This contribution deals with the history of the development of a new deposition technique based on spray-gun technology. At the very beginning, this technique was developed in 2006 in order to fabricate Carbon Nanotubes based Field Effect Transistors (CNTFETs) for gas sensing applications. Thanks to it, we were able to fabricate hundreds of operational devices, in a reproducible way, that were integrated in a chip. Following this first implementation, we decided to widen the application field of the deposition technique to energy and specifically to supercapacitors. In this context, we demonstrated in 2012 the fabrication of nanostructured electrodes for supercapacitors using mixtures of graphene/graphite and CNTs raising the capacitance and the power delivered by the device compared to barely CNTs based EDLC. Indeed, with high quality graphene we were able to reach a value of around 100W/Kg, which is very high value considering that it has been obtained with an industrially suitable technique. This dynamic spray-gun deposition has been also exploited for the fabrication of Resistance based Random Access Memories (ReRAM) based on thin layers of graphene oxide (GO) and of oxidized carbon nanofibers. In the first case, 5000 cycles of “write” and “read” phases were demonstrated. These results pave the way for the fabrication of very low cost memories that can be embedded in smart-cards, patches for health monitoring (e.g. diabetes), ID cards, RFID tags and more generally smart packaging. Finally we are also working on the utilization of this technique for the fabrication of conformable layers for Electro-Magnetic Shielding application. Thanks to a new machine with four nozzles, developed in the frame of the Graphene Flagship project, we are able to deposit four different nanomaterials at the same time or alternatively on a large surface creating specific nano-structuration and therefore ad-hoc architectures allowing the smart absorption of specific frequencies (e.g. X-band). All these applications demonstrate the extreme versatility of this technique that constitutes a real breakthrough for exploiting the nanomaterials characteristics

1  
2  
3 in real devices using an industrial suitable fabrication method that can be implemented using  
4  
5 roll-to-roll technique, as it is happening for the supercapacitors in the frame of the Graphene  
6  
7  
8  
9  
10  
11  
12  
13  
14  
15  
16  
17  
18  
19  
20  
21  
22  
23  
24  
25  
26  
27  
28  
29  
30  
31  
32  
33  
34  
35  
36  
37  
38  
39  
40  
41  
42  
43  
44  
45  
46  
47  
48  
49  
50  
51  
52  
53  
54  
55  
56  
57  
58  
59  
60

Flagship project.

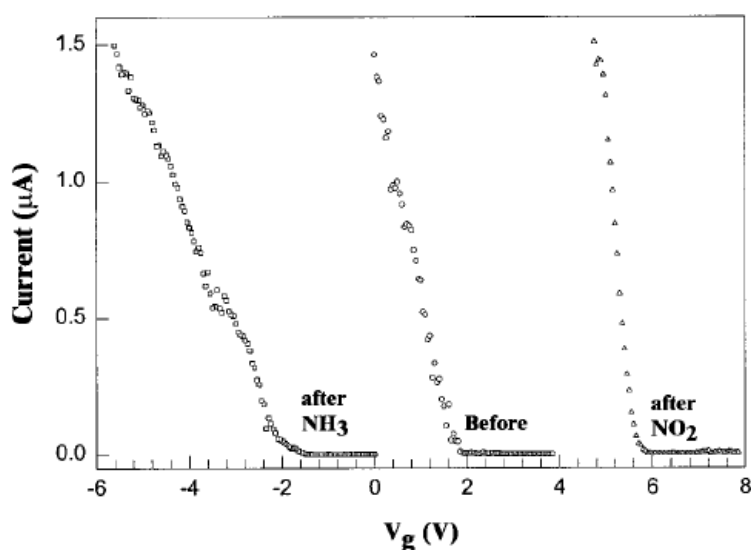
## Introduction

The discovery of nanomaterials and of their extraordinary physical/chemical properties has deeply changed the way we deal with material science. Thanks to their properties we can dramatically improve the performances of devices having a strong impact in our everyday life, reducing their dimensions and increasing the level of integration, while adding more functionalities. However, a big issue was rapidly pointed out: how to implement the properties of nanomaterials in a suitable and reproducible way, in order to make a real impact on the performances of “macro”-devices. Indeed, since the beginning, research teams have been focusing their efforts mainly on the study of the nano-objects by themselves, neglecting the potential issues related to their integration in real devices and systems. Our approach has been pragmatic and we have decided to take into account from the very beginning the fabrication method. The objective was to succeed in creating, designing and fabricating devices that can move from the dream realm to reality and therefore to real products. In this contribution, we discuss the development of a new deposition method for nanomaterials, based on the dynamic spray of suspensions of nanomaterials in specific solvents on large surface areas, with the possibility to implement it through roll-to-roll method. We show how we have conceived the fabrication method in parallel with the study of the nanomaterials properties and how these two aspects are both essential and can lead to effective innovations for devices. We focus our contribution on four main applications: gas sensors using carbon nanotubes based field effect transistors (CNTFETs), supercapacitors based on mixtures of carbon nanotubes (CNTs), carbon nanofibers (CNFs) and graphene, non-volatile ReRAM (Resistance Random Access Memories) making use of graphene oxide and oxidized carbon nanofibers (ox-CNFs) and finally Electromagnetic Interference (EMI) shielding layers based on graphene related materials, that is a new activity. All those four applications have been implemented using the dynamic spray-gun deposition technique. We also show how this

1  
2  
3 technique has evolved moving from a hand-operated technique for small surface areas to a  
4 completed automatic technique with potential for roll-to-roll fabrication in around ten years.  
5  
6 This contribution demonstrates how basic research on nanomaterials can promote real  
7  
8 advancements in terms of technological developments and yield devices that can be  
9  
10 integrated in existing systems if the fabrication issues are taking into account from the very  
11  
12 beginning.  
13  
14  
15  
16  
17

### 18 CNTFETs gas sensors

19  
20  
21 In 2004, within the frame of the Nanocarb lab at Thales Research and Technology (joint lab  
22  
23 between Ecole Polytechnique and Thales), we decided to develop a new concept of carbon  
24  
25 nanotubes field effect transistors (CNTFETs) for gas sensing applications. The first research  
26  
27 paper on CNTFETs used as gas sensor was published by Kong *et al.* at Stanford in 2000<sup>i</sup>. In  
28  
29 this pioneering study, the transistor channel was constituted by a single Single-Walled-  
30  
31 Carbon-Nanotube (SWCNT). The CNTFET was exposed to air, NH<sub>3</sub> and NO<sub>2</sub> and its transfer  
32  
33 characteristics (i.e., the variation of the current between drain and source as a function of the  
34  
35 gate bias) were observed to change as a function of the type of gas as shown in the Fig.1.  
36  
37  
38  
39  
40



1  
2  
3 ***Fig. 1: Transfer characteristic change after exposure to NO<sub>2</sub> and NH<sub>3</sub> of the first CNTFET***  
4 ***gas sensor fabricated at Stanford in 2000 by Kong et al.<sup>i</sup> . Gas-sensing experiments were***  
5 ***carried out by placing CNTFETs into a sealed glass flask and exposing to NO<sub>2</sub> ,2–200***  
6 ***parts per million (ppm), or NH<sub>3</sub> (0.1–1%) in Ar or air (flow rate of 700ml/min). The***  
7 ***channel length was around 5μm (Reproduced courtesy of AAAS) .***  
8  
9  
10  
11  
12  
13  
14

15 The interaction of gases with the CNT was interpreted as strictly connected to a bulk doping  
16 effect. However, some years later it was highlighted by different studies that the main effect,  
17 for channels shorter than 100μm, was on the work function of the metal contacts, which was  
18 shifted by the gas molecules<sup>ii,iii,iv,v,vi</sup>. This was at the origin of the change of the transfer  
19 characteristics of the CNTFETs. A lot of other works in the field followed, exploiting the  
20 same transistor configuration. The main common issue of all these contributions was to  
21 correctly achieve the contact between the CNT and the drain and source electrodes. This  
22 issue had already affected the development of CNTFETs for logic gates by IBM at the end of  
23 the 90ies<sup>vii,viii,ix,x,xi</sup> considering the difficulties to achieve ohmic-type contacts. In our case, we  
24 focused our efforts on CNTFETs achieved using mats of percolating SWCNTs. Indeed it had  
25 been demonstrated by previous theoretical studies, that exploiting the percolation of a layer of  
26 SWCNTs with larger concentration of semiconducting specimens compared to metallic ones,  
27 it was possible to obtain an overall semiconducting behavior<sup>xii,xiii</sup>. Thanks to that these mats  
28 can be used as transistor channels. Moreover, as demonstrated by Furher *et al.* in 2000<sup>xiv</sup>, the  
29 percolating chains linking the electrodes are composed only by semiconducting SWCNTs.  
30 Actually, Furher and co-workers evaluated the resistance of the contact between two metallic  
31 SWCNTs (MM), two semiconducting (SS) and of one semiconducting and one metallic one  
32 (SM). Experimentally they found a resistance of SM contacts twofold compared to SS or  
33 MM because the moving charges experienced tunneling between the two SWCNTs, as in  
34 case of SS and MM, but also a Schottky barrier linked to their different electronic character.  
35  
36  
37  
38  
39  
40  
41  
42  
43  
44  
45  
46  
47  
48  
49  
50  
51  
52  
53  
54  
55  
56  
57  
58  
59  
60

1  
2  
3 Considering that statistically the concentration of metal SWCNTs is largely lower than the  
4 concentration of semiconducting ones, the consequence is that only semiconducting chains  
5 bear the current between the two contacts. The main advantages of exploiting SWCNT-based  
6 mats compared to single carbon nanotube FETs, are therefore:  
7  
8  
9  
10

- 11 • The possibility to collectively fabricate arrays of transistors
- 12
- 13 • The process to fabricate the devices can be low cost and implemented on large  
14 surfaces.
- 15
- 16 • The electrical characteristics are the results of the average of the effect of several  
17 SWCNTs contacts on the electrodes. Thanks to this averaging effect, the final  
18 performances are more reproducible and do not depend anymore on the characteristics  
19 of each single SWCNT/metal contact.  
20  
21  
22  
23  
24  
25  
26  
27  
28  
29

30 In this context in 2006, we conceived and defined a new technology based on dynamic spray-  
31 gun deposition of the nanomaterials on 2” substrates, with pre-patterned electrodes, to  
32 fabricate arrays of hundredths of CNTFETs exploiting SWCNTs mats as channels for gas  
33 sensing application. To achieve uniform depositions, a new process needed to be developed,  
34 together with a new machine that could move the spray-gun on three axes and deposit the  
35 nanomaterials on a substrate. The SWCNTs used were supplied by SouthWest  
36 NanoTechnologies, and were CoMoCat SG65 composed by 90% of semiconducting  
37 SWCNTs. In order to obtain stable suspensions to be sprayed, we employed N-methyl-  
38 pyrrolidone (NMP) as solvent<sup>xv,xvi</sup>. SWCNT bundles and residual impurities (e.g., catalyst  
39 particles) were eliminated from the original SWCNT suspension. This was accomplished by  
40 sonication using a probe to “break” the bundles (1 h), followed by centrifugation (two phases  
41 of 10 min at 3000 rpm) and careful recuperation of the supernatant part of the suspension.  
42  
43  
44  
45  
46  
47  
48  
49  
50  
51  
52  
53  
54  
55  
56  
57  
58  
59  
60

dimension  $<100\mu\text{m}$ , reached the substrate that was heated at a temperature larger than the boiling point of the solvent, avoiding the so-called “coffee-ring effect”<sup>xvii, xviii</sup>. Indeed, the dispersed nanomaterials in a specific solvent tend to move to the borders of the droplet, when they are deposited by spray, if it dries at ambient temperature. This is related to the capillary flow induced by the differential evaporation rates across the drop (see fig.2): liquid evaporating from the edge is replenished by liquid from the interior.

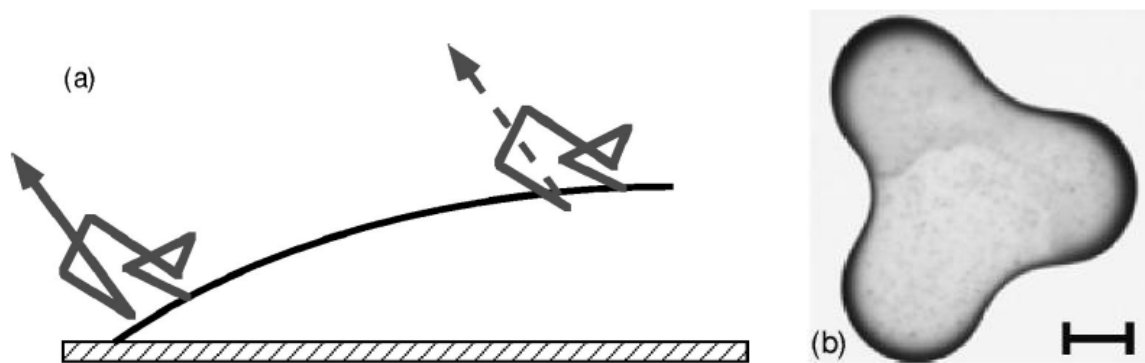


**Fig.2. a) Schema showing the probability of escape of an evaporating molecule as a function of its position in the drop. The evaporation rate is larger at the edge. b) Example of a typical coffee-ring shape where the boundaries of the drop exhibit the darkest deposits. The scale bar is approximately<sup>xvii, xviii</sup> (Reproduced courtesy of APS)**

For this reason, after drying completely, a pattern of concentric rings is observed. As a consequence, the final deposition is not uniform and not reproducible. To avoid this phenomenon, the substrate was heated to a temperature that allows instantaneous vaporization of the drops in contact with the substrate, avoiding the migration of nanomaterials to the borders of the drops. Thanks to that, the nanomaterials are stuck at the contact point. However, the substrate temperature had to be precisely adjusted to prevent droplets vaporization before reaching the substrate, which would reduce dramatically the final yielding of the deposition. Here, the yielding is defined as the ratio between the weight

of the nanomaterials in the suspension and the weight of the nanomaterials effectively deposited on the substrate. This method, patented<sup>xxi,xx</sup>, allowed us to fabricate wafers of CNTFETs with reproducible performances and with on/off current ratios of at least three orders of magnitude<sup>xxi</sup>. Indeed, to perform a selective sensing we decided to fabricate an array of sensors composed by different metals as contacts (see patent<sup>xxii</sup>). Actually, considering that the detection is based on the effect of gases on the Fermi Level between the metal contacts and CNTs, and that each metal has a different working function, the gas changes in a very specific way the transfer characteristics of the CNTFETs as a function of the nature of the metal. Thanks to that we are able to achieve an electronic fingerprinting of the gas after exposure to the array of CNTFETs. In fig.3, the response of an array composed by CNTFETs with four different metals (Au, Pd, Ti, Pt) as contacts is shown after exposure to NO<sub>2</sub><sup>iii</sup>.

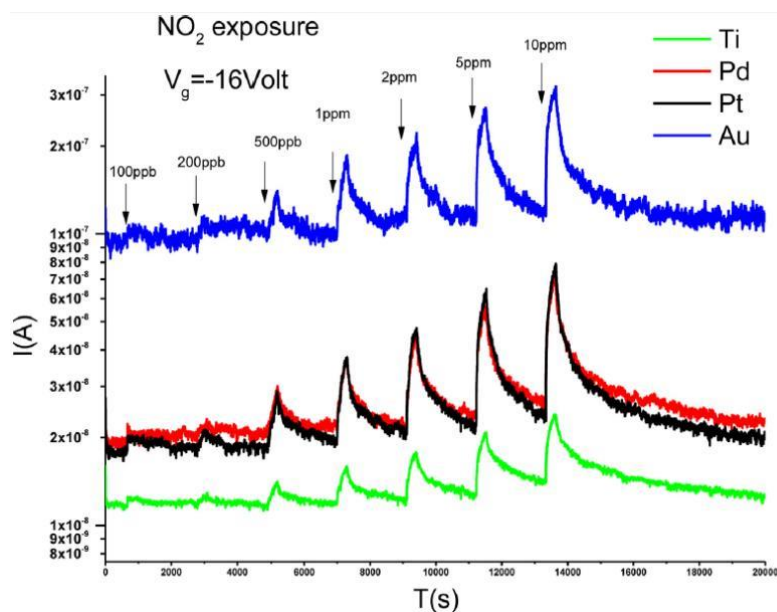


**Fig.3. Change of the  $I_{DS}$  current (D and S, respectively stay for Drain and Source) as a function of time for  $V_{GS} = -16$  V (G stays for Gate) and  $V_{DS} = 1.6$  V for concentrations between 100 ppb and 10 ppm of NO<sub>2</sub>. The exposure time to NO<sub>2</sub> is of 300s and to air of 600 s<sup>iii</sup> (Reproduced courtesy of Elsevier).**

1  
2  
3 Thanks to the good results obtained, an array of transistors was integrated on a final chip for  
4 gas sensing utilization (see fig.4). The data obtained during the measurements were recorded  
5 by a specific data treatment module in order to perform a selective detection reducing the  
6 false alarm rate and to avoid the environment gases influence on the final response. The  
7 success of the exploitation of the dynamic spray-gun deposition method in this activity  
8 motivated our team to implement its application in other fields, as in case of the fabrication of  
9 energy storage devices.  
10  
11  
12  
13  
14  
15  
16  
17  
18  
19  
20

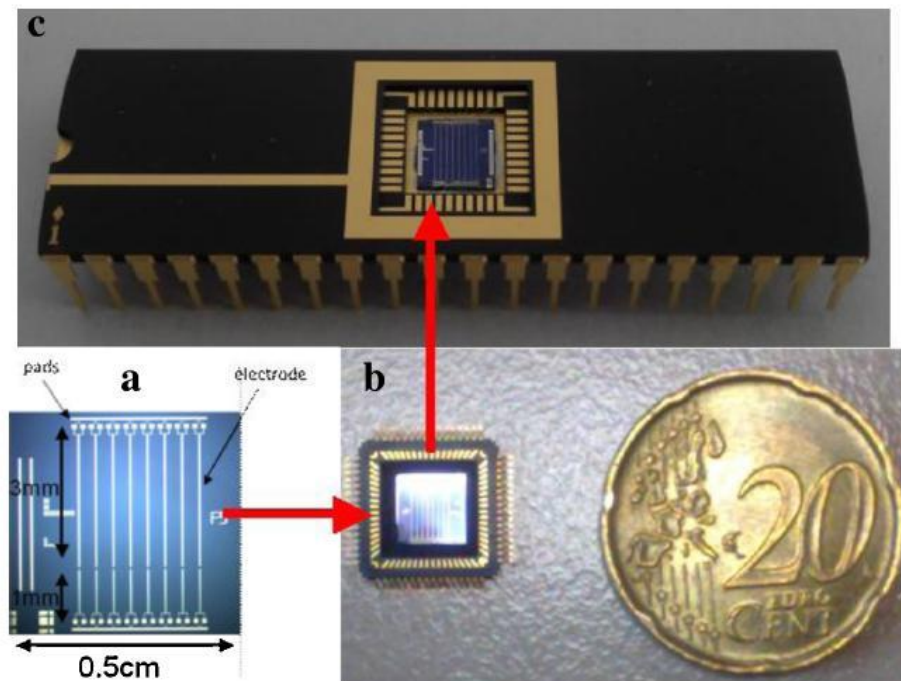


*Fig. 4. (a) Chip containing 16 CNTFETs achieved using four different metals as electrodes (four for each metals), (b) Chip dimensions compared to a 20 cents coin, (c) Chip mounted on the C-DIL used for tests<sup>iii</sup>. (Reproduced courtesy of Elsevier)*

### **Application to the energy field: supercapacitors based on mixtures of graphene and CNTs**

The versatility of the deposition technique by dynamic spray pushed us to exploit it for the fabrication of supercapacitors also called Electro-Double-Layer-Capacitors (EDLC). One of

1  
2  
3 the first papers showing that spray could be used to fabricate this kind of devices was  
4 published by Kaempgen *et al.* in 2009<sup>xxiii</sup>. In this case, Kaempgen and co-workers fabricated  
5 thin film supercapacitors with sprayed networks of SWCNTs, which were in water  
6 suspension with specific surfactant, serving both as electrodes and charge collectors.  
7 Specifically, with a static spray-gun, the stable suspension was deposited onto polyethylene-  
8 terephthalate (PET) substrates placed on a hot plate. During spraying, the water was  
9 evaporated and the SWCNTs formed an entangled random network on the PET without any  
10 other treatment. The mass of the SWCNTs coated on each substrate was determined by  
11 weighing the PET before and after the deposition. All SWCNT films used typically had a  
12 sheet resistance of  $\sim 40\text{-}50 \text{ }\Omega/\text{m}^2$  and a thickness of  $\sim 0.6 \text{ }\mu\text{m}$ . This thickness was extremely  
13 small considering that in commercial supercapacitors the thickness is of the order of  $\sim 100\text{ }\mu\text{m}$ .  
14 Even though these devices were not yet optimized, mainly in terms of the electrical  
15 conductivity and thickness of the CNTs based films, their performance already spanned the  
16 typical range of conventional supercapacitor devices for all electrolytes used. This was  
17 achieved thanks to the increased effective surface area in the thin films, maximizing the  
18 efficiency of the supercapacitors, compared to the thick activated carbon electrodes in regular  
19 devices. Moreover, the simplified architecture had the potential to lead to a new class of light,  
20 flexible and printable charge storage devices. In 2011, Cheng *et al.*<sup>xxiv</sup> demonstrated the  
21 interest of using mixtures of graphene and CNTs to achieve nanostructured electrodes.  
22 Thanks to that, Cheng and co-workers managed to increase the overall surface area to store  
23 charges, and so the density of energy, using the CNTs as spacers, thus preventing the  
24 restacking of the graphene flakes (and so the loss of effective surface). At the same time, this  
25 mixture also allows creating a mesoporous distribution inside the electrode that could  
26 improve the power delivered. In fact, the term 'mesoporous' is used to highlight a pore  
27 distribution with pore sizes that can vary between 2 and 50nm. A mesoporous distribution  
28  
29  
30  
31  
32  
33  
34  
35  
36  
37  
38  
39  
40  
41  
42  
43  
44  
45  
46  
47  
48  
49  
50  
51  
52  
53  
54  
55  
56  
57  
58  
59  
60

1  
2  
3 constitutes a favorable pore network that fits the charge dimensions and therefore can  
4 improve the circulation of the ions inside the electrodes. As a result, a very fast charge and  
5 discharge of the device can be achieved. In 2012, exploiting our spray-gun deposition  
6 technique, we decided to fabricate mixtures of partially exfoliated graphite and Multi-Walled-  
7 Carbon-Nanotubes (MWCNTs)<sup>xxv</sup>. Graphite (ref 332461) and MWCNT (ref 724769-25G)  
8 powders were purchased from Sigma Aldrich. Both powders were dispersed in N-Methyl  
9 Pyrrolidone (NMP) at concentrations of 0,5mg/mL. MWCNT-based solutions were sonicated  
10 for 10 minutes at high power (Vibra-cell 75185 by Sonics, 130 W). In case of the partially  
11 exfoliated graphite flakes, to prevent their destruction, we sonicated them during 18 h in a  
12 low power sonic bath (Branson 1510E-MT bath sonicator, 70 W). No centrifugation was  
13 performed after dispersion, whether CNT or graphite suspensions were concerned. The  
14 graphite and CNT suspensions were then mixed in 5 different volume ratios (0%, 25%, 50%,  
15 75% and 100%) to obtain different proportions. In this way we wanted to identify the best  
16 compromise to achieve the more effective electrode in term of specific capacitance and  
17 power. Since both dispersions had the same solid concentration (0.5mg/mL), the resulting  
18 mixtures also had the same solid concentration. The 5 final mixtures were further sonicated  
19 for 18 h in the low power sonic bath to improve the entanglement of the nanomaterials. The  
20 final stable suspensions were then gun-sprayed on graphite collectors (graphite foil,  
21 EYGS182307, Panasonic) at a constant distance of ~15 cm from the surface. In their paper,  
22 Cheng *et al.* obtained the electrodes by fabricating bucky papers through complex filtration  
23 steps. This technique clearly cannot be scaled-up and it is mainly used to fabrication of lab  
24 samples. In our case, the main advantage is that we could perform the uniform deposition on  
25 relatively large surface electrodes (15cmx15cm) with the possibility of implementation on  
26 roll-to-roll (see next sections). The results of these first tries were very promising in terms of  
27  
28  
29  
30  
31  
32  
33  
34  
35  
36  
37  
38  
39  
40  
41  
42  
43  
44  
45  
46  
47  
48  
49  
50  
51  
52  
53  
54  
55  
56  
57  
58  
59  
60

1  
2  
3 power density ( $\sim 40\text{kW/Kg}$ ) thanks to the nanostructuration that we were able to achieve with  
4  
5 our deposition technique (see fig.6).  
6  
7

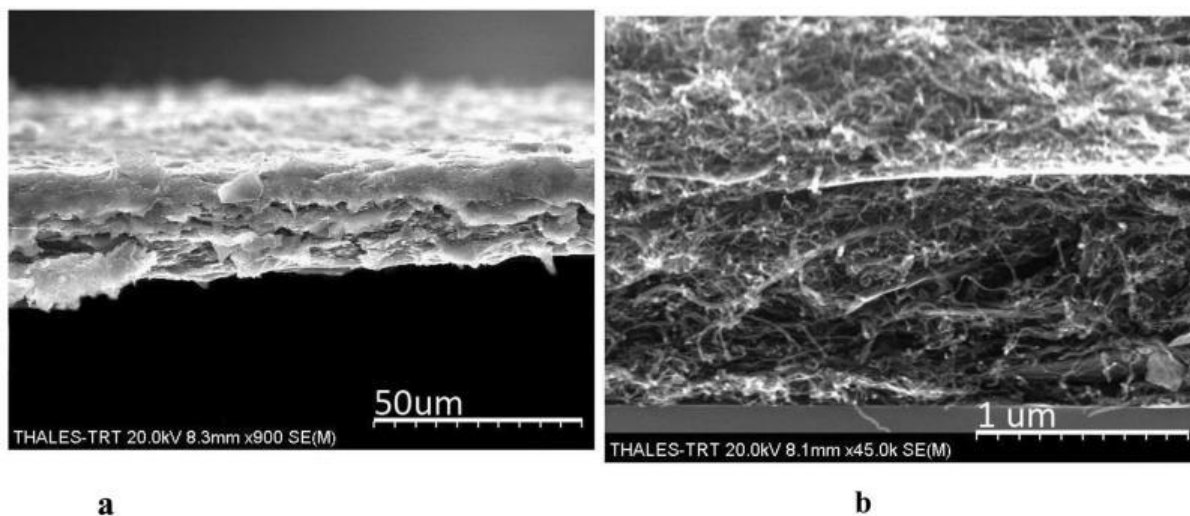


**Fig.6. SEM pictures of the cross section of a graphite collector with an electrode deposited by the spray gun method and composed of a mixture of graphene/graphite(50%)/CNTs(50%). (a) overall view of the cross section, (b) detailed view of the surface of the sample<sup>xxv</sup> (Reproduced with permission from *J. Electrochem. Soc.*, 150, H205 (2003). Copyright 2003, The Electrochemical Society).**

In Fig.6, the intercalation of the CNTs between the layers of graphene/graphite can clearly be observed. The most interesting results showed that when we use mixtures of 75% of Graphene/Graphite and 25% of CNTs we get the best performances in terms of power delivered which is around 2.5 times larger than the case of electrodes fabricated using only CNTs. This seemed to be the best concentration that allows achieving the best pore distribution.

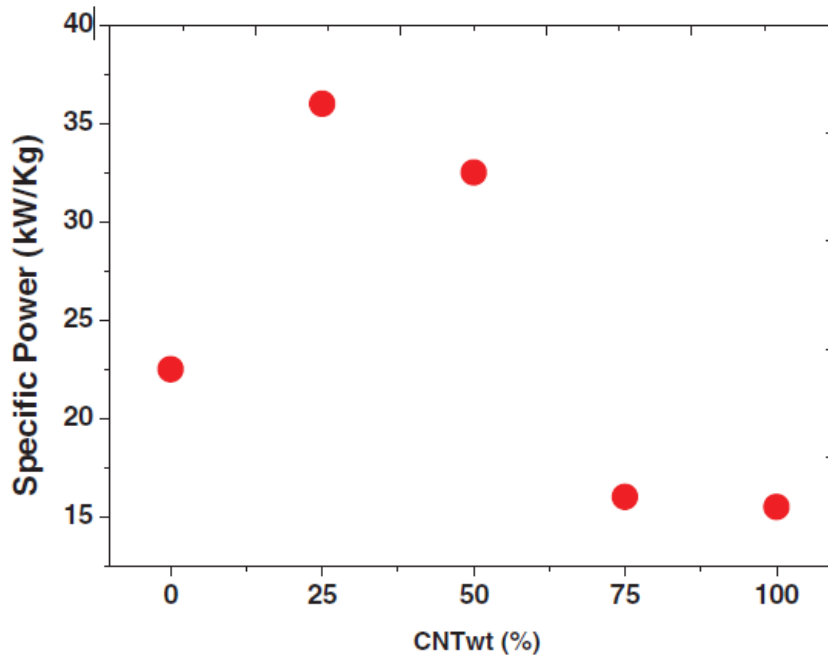


**Fig.7: Specific power of a cell fabricated using electrodes characterized by different concentrations of CNTs. The weight of each sample was 1.80 mg (+/-0.02 mg), the surface 2 cm<sup>2</sup> (coin cell) and the thickness around 20  $\mu\text{m}^{\text{xxv}}$  (Reproduced with permission from *J. Electrochem. Soc.*, 150, H205 (2003). Copyright 2003, The Electrochemical Society).**

These preliminary results were dramatically improved in 2017 using mixtures of high quality exfoliated few layer graphene (supplied by IIT) and SWCNTs<sup>xxvi</sup>. The few layer graphene flakes were produced by liquid phase exfoliation (LPE) after mixing 20g of graphite (Sigma-Aldrich, flakes) with 1L of NMP (Sigma-Aldrich, purity 99%). The exfoliation was performed by bath sonicator (VWR) for 6 hours and then ultracentrifuged at ~12300g (10k RPM in a Beckman Coulter Optima™ XE-90 with a SW32Ti rotor) for 30 min at 15 °C, to exploit sedimentation-based separation. The supernatant was then collected by pipetting, obtaining a SLG/FLG flakes-based dispersion. Concerning the SWCNTs, the powder (BuckyUSA, BU-203, purity 95% in weight, length 0.5- 5  $\mu\text{m}$ , diameter 0.7-2.5 nm) was used as received (without any purification step). SWCNTs were dispersed in NMP at a

concentration of 0.5 mg/ml by sonicating the dispersion for 10 minutes at high power (0.625 W/ml, Vibra-cell 75185 by Sonics). The two suspensions were mixed together and sprayed on a graphite-based collector. The devices were assembled using 2 cm<sup>2</sup> area electrodes and a common aqueous electrolyte (3M LiNO<sub>3</sub>) to build a coin cell. This architecture allows us to effectively balance the supercapacitors performance achieving gravimetric capacitance, specific energy and power of 104 F g<sup>-1</sup>, 20.8 Wh kg<sup>-1</sup>, and 92.3 W kg<sup>-1</sup>, respectively.

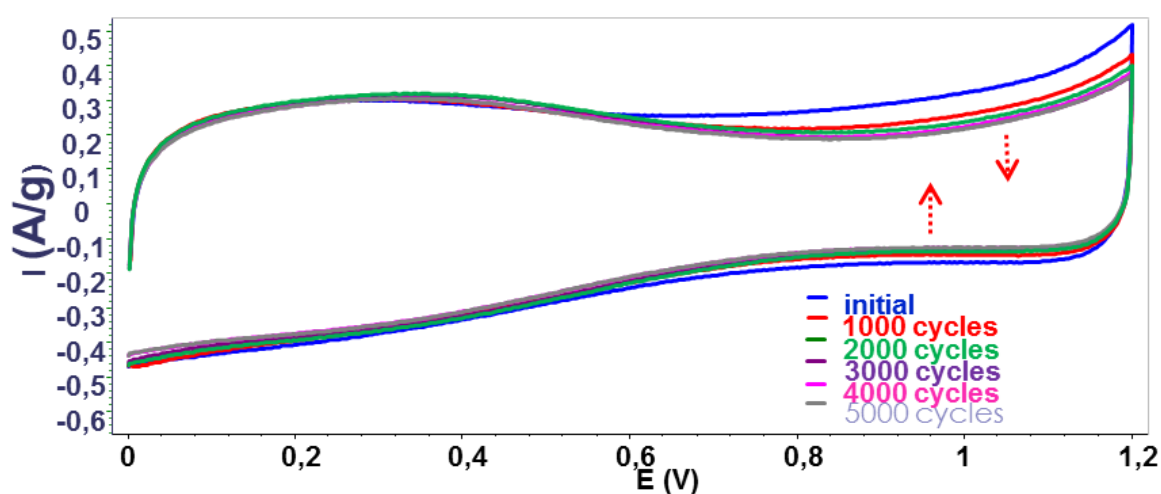
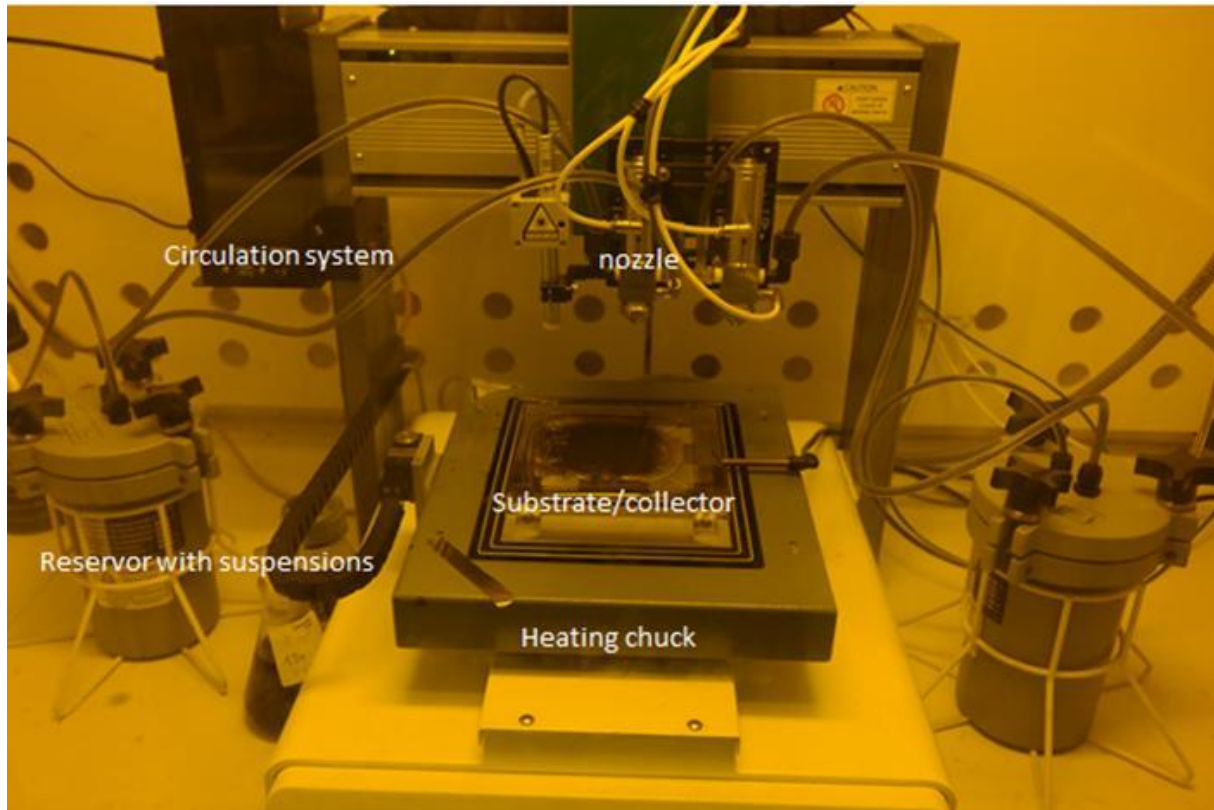


**Fig.8:** Cyclic voltammetry plots performed on the symmetric EDLC every 1000 cycles showing the current fading over time.

In Fig.8, we can see that the supercapacitor cells were cycled up to 5000 cycles without any strong deviation after the first 2000. These results, based on industrially scalable materials production and deposition method, represent a real breakthrough compared to state-of-the-art lab-scale devices. Since 2017, at Thales Research and Technology, we have worked on the development of a new machine with two nozzles (see Fig.9). Thanks to that we have been able to fabricate finely tuned multilayered structures to improve the EDLC performances. Indeed, with this new machine, it is possible to deposit, in an alternate way, layers of two different nanomaterials and therefore to fabricate nanostructured architectures in a more

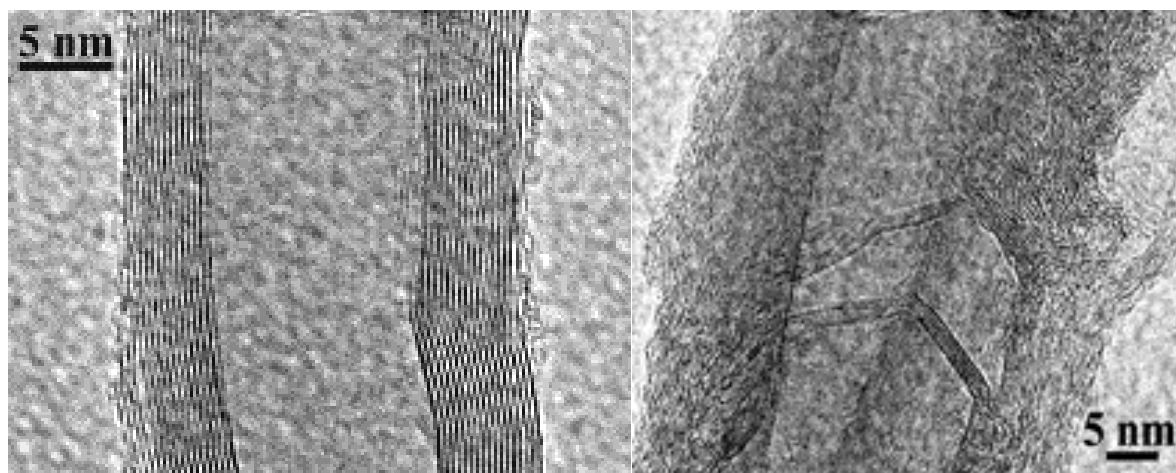
1  
2  
3 deterministic way. Considering that the samples for EDLC fabrication are largely thicker  
4 (tens of  $\mu\text{ms}$ ) than the layers needed for gas sensors applications (some nms), using the one  
5  
6 nozzle machine, we faced some problems concerning the clogging of the spray-gun. In the  
7  
8 new machine we decided to integrate a circulation system (see Fig.9) in the nozzles to avoid  
9  
10 this issue and also to keep the suspensions always in movement, to prevent sedimentation.  
11  
12  
13  
14



41  
42  
43 ***Fig.9. Dynamic Spray-gun set-up developed at Thales in 2017.***  
44

45  
46 Using this new machine, we have also worked on mixtures of graphene and CNFs. CNFs  
47  
48 differ in relation to CNTs mainly on their structure, since for CNFs a cone angle between the  
49  
50 graphite basal planes and the tube axis exists, which leads to the absence of the concentric  
51  
52 structure that CNTs have. Due to this difference, CNFs appear to be compact sometime, in  
53  
54 contrast with CNTs that have a hollow structure. The most important difference however,  
55  
56 taking into account the spray-gun application, is their diameter difference; CNFs tend to be  
57  
58  
59  
60

1  
2  
3 thicker, compared to CNTs. The following TEM images present the main structural alteration  
4  
5 between CNTs and CNFs (Fig.10):  
6  
7



25 **Fig. 10: TEM images of CNT (left) and CNF (right) internal structure**

26  
27  
28 Considering that CNTs and CNFs are used as sort of spacers between the graphene layers it is  
29 clear that using CNFs, with diameters between 50-100nm we can optimize the porous  
30 distribution for ionic liquid utilization. Such electrolytes have been developed to fabricate  
31 supercapacitors that are able to withstand harsh environments, in a range of temperatures  
32 between - 40°C and +100°C for avionics application. There are no existing EDLCs able to  
33 satisfy these specifications up to now. One of the main characteristics of ionic liquids is the  
34 average larger size of charge carriers. Moreover, viscosity of ionic liquids markedly increases  
35 at low temperature. As a consequence, to keep an acceptable value of the power delivered, we  
36 need to have a well interconnected network of pores, with a larger size compared to aqueous  
37 electrolytes used in the previous works (see Fig.12). Compared to the previous results the  
38 structures were fabricated in a more deterministic way, as mentioned above, alternating layers  
39 of graphene, in this specific case Reduced Graphene Oxide (RGO) from Graphenea, and  
40 CNFs grown by the National Technological University of Athens (NTUA) with a length of  
41 around 10 $\mu$ m and diameter of around 100nm. CNFs were synthesized through the Thermal  
42  
43  
44  
45  
46  
47  
48  
49  
50  
51  
52  
53  
54  
55  
56  
57  
58  
59  
60

Catalytic Chemical Vapour Deposition (TC-CVD) method, by the supported catalyst approach. By this, tailored properties of the CNFs can be achieved, through the careful selection of the catalyst and the experimental conditions (temperature range, flow rate of the reaction gases, reaction atmosphere and duration, substrate, etc.). In Fig. 11 a SEM image of the used CNFs is presented:

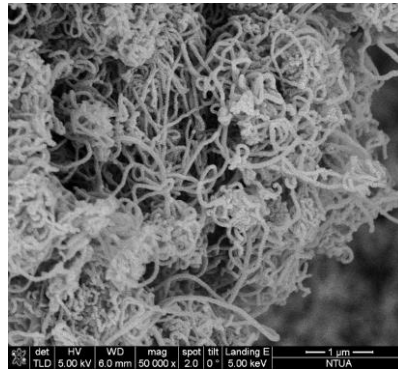
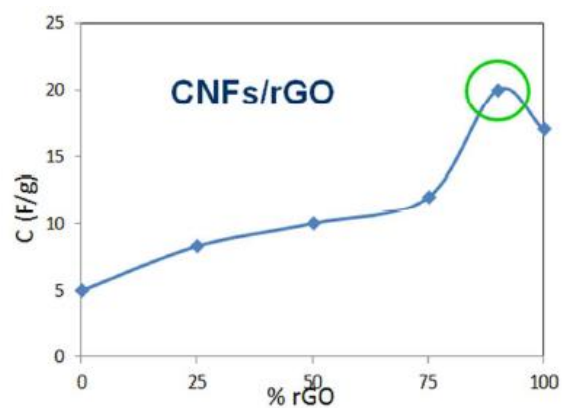
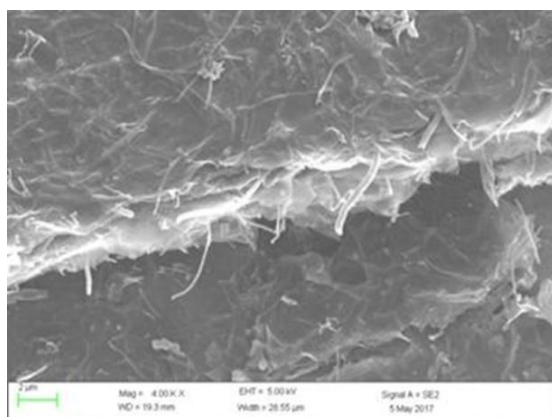


**Fig. 11: SEM image of CVD produced in the National Technical University of Athens (R-Nano Lab)**

The results showed that the best compromise in terms of capacitance was obtained for a concentration of 90% of RGO (20F/g) with a power delivered of 40kW/Kg. This last value is at the state of the art for devices using ionic liquids and able to afford the interval of temperature mentioned above.



1  
2  
3 *Fig.12: Left: SEM images the cross section of the deposited layers after deposition of*  
4 *mixture of CNFs and RGO. Right : Capacitance of a supercapacitor cell fabricated with*  
5 *two electrodes achieved with mixing of RGO and CNFs at different concentrations. The*  
6 *best results are obtained with a concentration of 90% of RGO and 10% of CNFs using*  
7 *ionic liquids as electrolytes*<sup>xxvii</sup>*(Reproduce courtesy of Materials Research Society 2018).*  
8  
9  
10  
11  
12  
13  
14

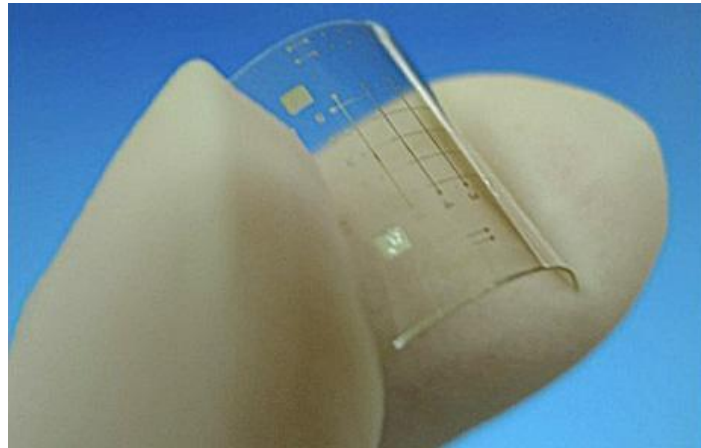
15 This last device was another evident example of the capacity to perform a nano-structuration  
16 exploiting our macro deposition technique avoiding complex and therefore non-industrially  
17 suitable processes that have no potential to be scaled-up.  
18  
19  
20  
21  
22

### 23 **Carbon based Non-volatile based memories by spray-gun deposition**

24  
25

26 Another extremely promising application that can be implemented by dynamic spray-gun  
27 deposition method is the fabrication of low-cost graphite based memories that might be  
28 integrated to flexible, plastic or paper based substrates<sup>xxviii</sup>. Indeed in the International  
29 Technology Roadmap for Semiconductors (ITRS) issued in 2011<sup>xxix, xxx, xxxi</sup>, it was stated in  
30 the chapter concerning Emerging Research Devices (i.e. ERD) and more specifically on  
31 memory devices, that ultrathin graphite layers were “interesting materials for macromolecular  
32 memories thanks to the potential fabrication costs that are considered as the primary driver  
33 for this type of memory, while extreme scaling is de-emphasized”. In fact, this kind of  
34 memories can be used for low-cost applications and integrated for example in ID cards,  
35 driver licenses, smart-cards or smart packaging in general. At the state of the art, there are no  
36 flexible, low-cost memories that have been integrated to existing systems. In our case we  
37 wanted to fabricate Metal-Insulator-Metal (MIM) structures where the graphene based  
38 materials were sandwiched between two contacts. This kind of structure is a Resistance  
39 Random Access Memory (Re-RAM)<sup>xxxii, xxxiii, xxxiv</sup> where the resistance of the sandwiched  
40 material is changed applying a bias between the top and bottom contact. One of the first work  
41  
42  
43  
44  
45  
46  
47  
48  
49  
50  
51  
52  
53  
54  
55  
56  
57  
58  
59  
60

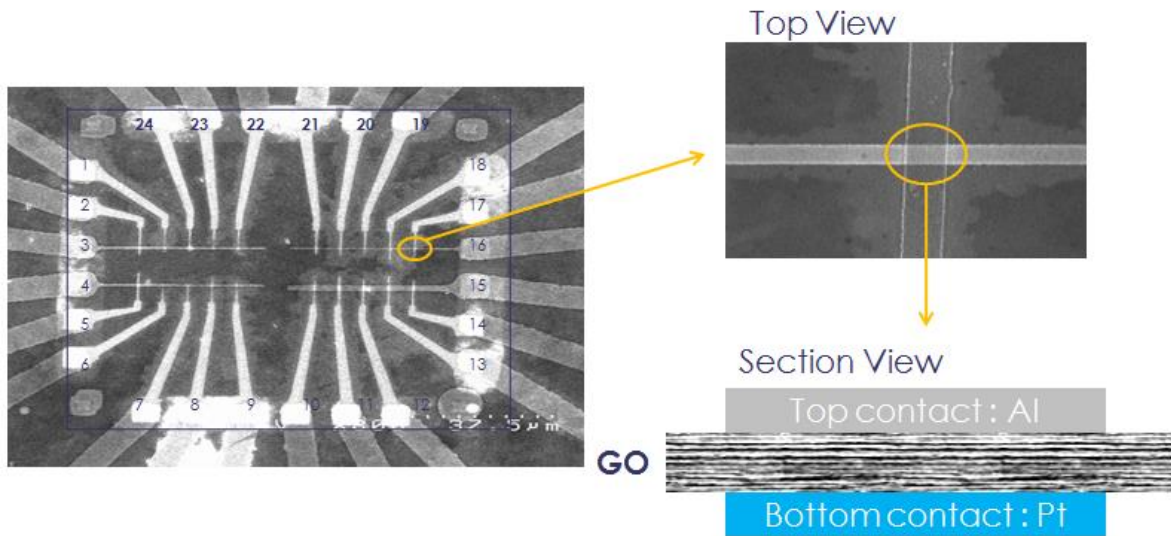
1  
2  
3 showing the utilization of graphene based mats for flexible non-volatile Re-RAM was  
4 published in 2010 by Jeong et al.<sup>xxxv</sup>. Thanks to its hydrophilic character, graphene oxide  
5 (GO) flakes were easily put in stable suspensions in water and deposited on large surface  
6 using spin coating process. This team demonstrated the non-volatile effect on the resistance  
7 of a 70nm layer thick of GO flakes in a layered structure composed by Al/GO/Al (see fig.13)  
8 exploiting a classic cross-bar configuration.  
9  
10  
11  
12  
13  
14  
15  
16  
17



18  
19  
20  
21  
22  
23  
24  
25  
26  
27  
28  
29  
30  
31  
32  
33 ***Fig.13: Flexible crossbar memory devices based on GO<sup>xxxv</sup> (reproduced courtesy of ACS)***

34  
35  
36 In this context, we can also mention the work of He et al. in 2009<sup>xxxvi</sup> where reliable and  
37 reproducible resistive switching behaviors were observed in GO thin films prepared by  
38 vacuum filtration method<sup>xxxvii</sup>, the common technique used to fabricate CNTs based bucky  
39 papers. The suggested physical principle at the origin of the switching effect was the  
40 absorption/desorption of oxygen-related groups on the GO sheets as well as the diffusion of  
41 the top electrodes. The alignment of the oxygen vacancies creates conducting paths that  
42 reduces the resistance of the sandwiched layers. Another hypothesis concerns the oxidation of  
43 the top contact. Hong et al.<sup>xxxviii</sup> performed a deep analysis of the switching mechanism for  
44 this kind of devices. They underlined that these structures had performances dependent on the  
45 origin of the top contacts. For example, in case of Au based top electrodes that cannot be  
46 oxidized, there was no oxygen migration in opposition to Al electrodes. Thanks to that we  
47  
48  
49  
50  
51  
52  
53  
54  
55  
56  
57  
58  
59  
60

1  
2  
3 move from a high resistance state (HRS) to a lower resistance state (LRS). These experiments  
4 underlined that GO was potentially useful for future non-volatile memory applications. In  
5  
6  
7  
8 2015, in a joint work with CEA (not published), we decided to fabricate GO based memories  
9  
10 using spray-gun deposition method. We achieved structures as show in fig.14 where the GO  
11  
12 were sandwiched between two metal contacts, with a thickness of tens of nanometers.  
13  
14  
15  
16  
17  
18  
19  
20  
21  
22  
23  
24  
25  
26  
27  
28  
29  
30  
31  
32  
33  
34



35 **Fig.14: Graphene based memories based on graphene oxide layers. At the left the**  
36 **overview of the device composed by 20 bottom contacts and 4 top contacts. The GO is**  
37 **sandwiched at the intersections creating MIM structures (work in collaboration with**  
38 **CEA).**  
39  
40  
41  
42  
43  
44

45 The structures obtained were cycled 100 times between “write” and “delete” phases showing  
46 also a very good ON stability during the “read” phase (5000 cycles) as highlighted in figure  
47 15. These results constitute the first example of graphene based memories achieved using  
48 spray-gun deposition method.  
49  
50  
51  
52  
53  
54  
55  
56  
57  
58  
59  
60

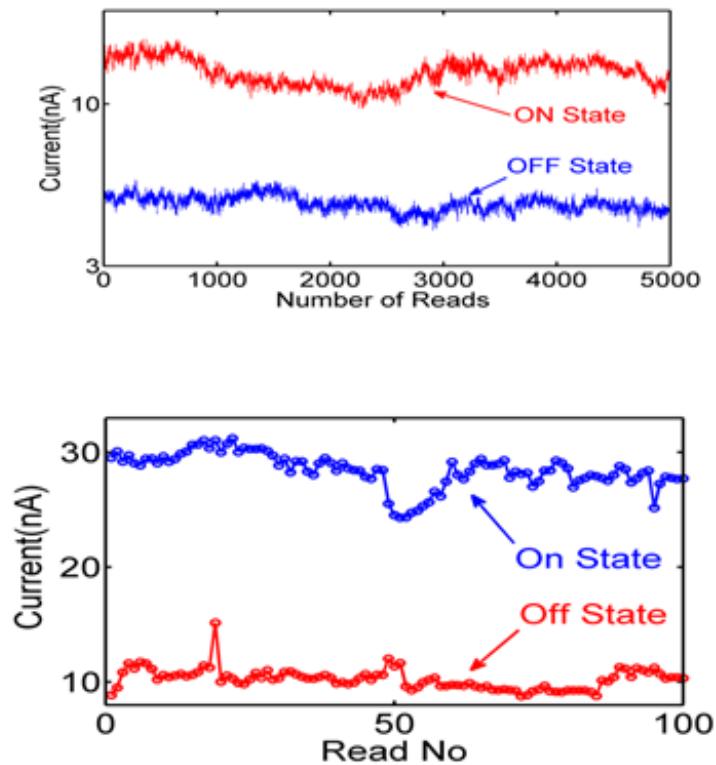


**Fig.15: Top: persistence of the on state after 5000 cycles of reading. Bottom: switching characteristics after 100 cycles of “write” and “delete” (work in collaboration with CEA).**

Starting from these preliminary results, we have decided to implement the possibility to fabricate memory based on oxidized carbon nanofibers (ox-CNFs) this taking into account that CNFs are less expensive and that graphene was only the “vehicle” of the oxygen atoms. Considering that the final thickness of the insulator layer had to be around 50nm we achieved extremely diluted suspensions using ox-CNFs in de-ionized water. After defining specifications for CNFs dimensions (diameters and length), National Technical University of Athens (in the frame of European H2020 NMP project MODCOMP<sup>xxxix</sup>) provided ox-CNFs to prepare stable suspensions to be sprayed. CNFs were purified to remove any amorphous by-product and the metallic catalyst residues that could be at the origin of the formation of dendrites between the two electrodes and so of the short-circuit and pinning of the device<sup>xl</sup>. In order to purify the sample, a step by step chemical procedure took place. Initially, the sample

1  
 2  
 3 was stirred in NaOH, to remove the ceramic substrate. Afterwards, the dried sample was  
 4  
 5 extracted with HCl in a Soxhlet apparatus. Washing took place with distilled water, in order  
 6  
 7 to remove the dissolved catalyst. Chemical functionalisation of their surface was carried out  
 8  
 9 with a strong acid treatment. By this, oxidation of their surface was achieved, since oxygen  
 10  
 11 groups were anchored (-COOH, -OH, =O). Considering that the CNFs are oxidised, we were  
 12  
 13 able to obtain extremely stable suspensions in water. This allowed us to develop a green-type  
 14  
 15 process and to reduce the heating temperature of the heating chuck that in case of NMP has to  
 16  
 17 be larger than 202°C and in case of water of only 100°C. The suspensions were obtained  
 18  
 19 using 10mg of ox-CNFs in 500ml of de-ionized water. We performed centrifugation during  
 20  
 21 20 minutes, in two phases, at 3000t/m. We removed only the top part of the suspensions that  
 22  
 23 was centrifuged. This step is very important in order to avoid utilisation of bundles which too  
 24  
 25 large thickness, a critical parameter for the final fabrication of the memories. The part of  
 26  
 27 removed suspensions is further diluted in 500ml of de-ionized water and sonicated in a bath  
 28  
 29 for 6 hours, after that we can perform the deposition on a 2" silicon based substrate that was  
 30  
 31 preliminary metallized using a Ti/Pt layer. On top of the deposited CNF layer, we patterned  
 32  
 33 100µm x 100µm squares where we deposited AlCu/Au contacts. The active memory stack is  
 34  
 35 depicted in fig.16a:  
 36  
 37  
 38  
 39  
 40  
 41  
 42  
 43  
 44  
 45  
 46  
 47  
 48  
 49  
 50  
 51  
 52  
 53  
 54  
 55  
 56  
 57  
 58  
 59  
 60

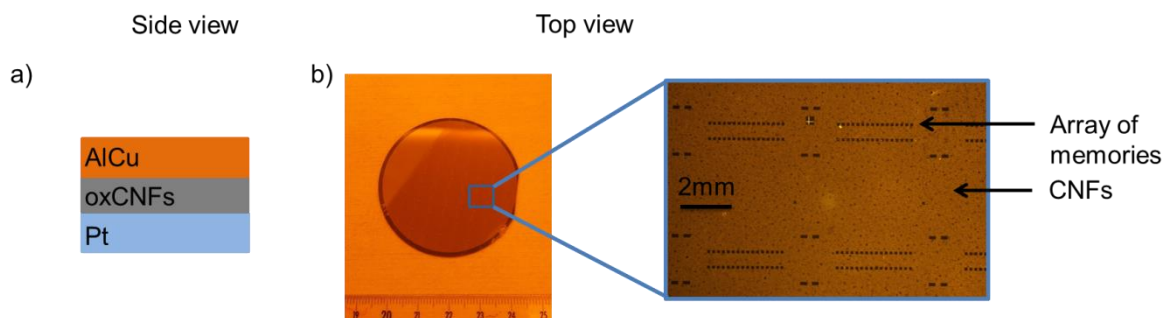


**Fig.16: Side and top views of the sample. a) cross-section of the structure b) top-view of sample and detail of the top contact of MIM-type devices.**

The ox-CNFs are in contact with the inert bottom electrode of Pt and the easy-oxidised top electrode of AlCu. By applying a positive voltage between the bottom and top electrode, the oxygen atoms migrate from the ox-CNF layer to the AlCu electrode. By applying the opposite voltage, the oxidised AlCu electrode gives back the oxygen atoms to the CNF layer. This back and forth of the oxygen atoms lead to a hysteretic change of the current shown on Fig 17.

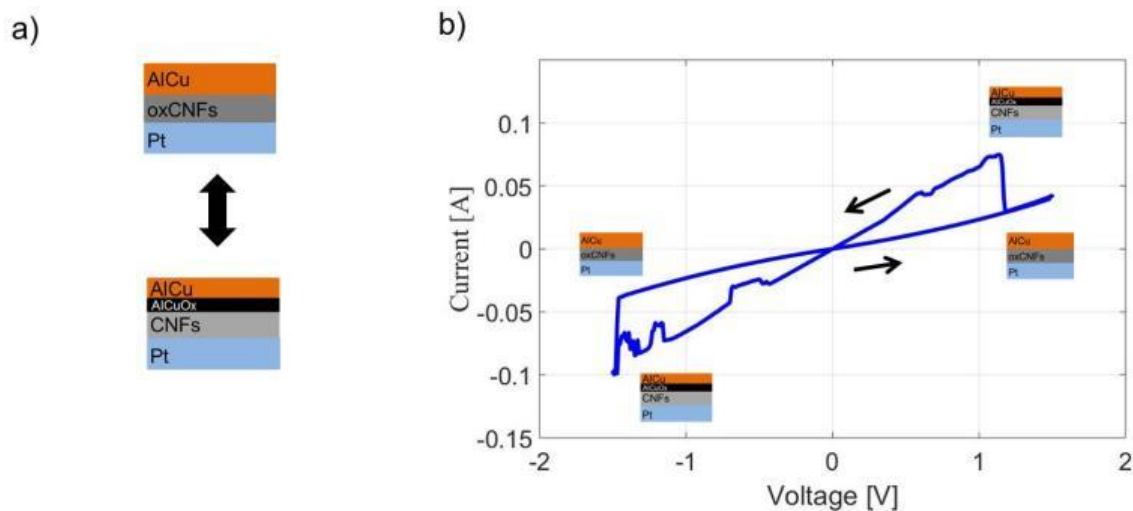


**Fig.17: a) Schematic side view of the two states of resistance of the memory stack b) Image of a cycle obtained by applying a voltage between the inert Pt electrode and the AlCu electrode. The hysteretic change of current results from the migration of oxygen atoms between the CNF layer and the AlCu metal.**

These very promising results obtained on a hard substrate demonstrate that memories can be fabricated using CNFs and pave the way to the revolution of memories on flexible substrates (already fabricated and to be tested in the following months), which at the moment do not exist as commercial components in the market. This will allow widening the implementation of low-cost memories in large market applications as ID cards, smart cards, memories for health monitoring on specific patches (e.g. diabetes monitoring), ticketing, smart packaging, etc...

### **Perspective for new applications (in progress): Electromagnetic Shielding**

Another potential application for dynamic spray-gun deposition method is the fabrication of layered structures to achieve smart reflection or absorption of specific frequencies, performing what is commonly called Electromagnetic Interference shielding (EMI)<sup>xli</sup>. As mentioned, two mechanisms of EMI coexist: one is based on reflection, the other on absorption. In the first case we want to achieve high conductivity layer thanks to spray gun deposition. Indeed, a solution to achieve high reflectivity is the use of metal for this application. The main issues are that metals are costly, they have high densities (so they are heavy) with corrosion susceptibility. With spray-gun deposition of conducting nanomaterials, the weight would be decreased but it would also be possible to manufacture conformable surfaces exploiting mixing of nanomaterials with polymers<sup>xlii,xliii,xliv</sup>. In case of shield exploiting absorption, it is necessary to have materials with electrical or magnetic dipoles. For this reason in this case materials with high dielectric constant (ZnO, SiO<sub>2</sub>, TiO<sub>2</sub>...) or high magnetic permeability (Ni, Co, Fe...) are exploited<sup>xlv</sup>. These materials are heavy and their manufacturing is complex. Composites could replace them but with reduction in performance. One of the solutions that we will suggest to explore using deposition by spray-gun is to fabricate layers of dielectric alternating layers of graphene. Thank to that we would like to build-up, exploiting the Maxwell-Wagner-Sillars (MWS) <sup>xlvi, xlvi, xlviii</sup>, polarization effect at the interface between the conductive materials (graphene sheets) and dielectric materials (e.g. polymers) architectures able to trap the charges. We can mention the work of Li et al.<sup>xlix</sup> where graphene sheets (GS)/polyacrylate (PA) composites favored the build-up of a segregated GS architecture stacked in the polymer matrix. This unique nanostructured GS architecture not only enhanced the electrical conductivity of composites, but also induce strong Maxwell–Wagner–Sillars (MWS) polarization at the highly conductive GS/non-conductive PA interfaces. The EMI shielding effectiveness (SE) of these composites was

enhanced with increasing GS content, and the composite with 6 wt% GS loading exhibited a high EMI SE of  $\sim 66$  dB over a frequency of 8.2–12.4 GHz, resulting from the pronounced conduction loss, dielectric relaxation, and multiscattering (see fig.18).

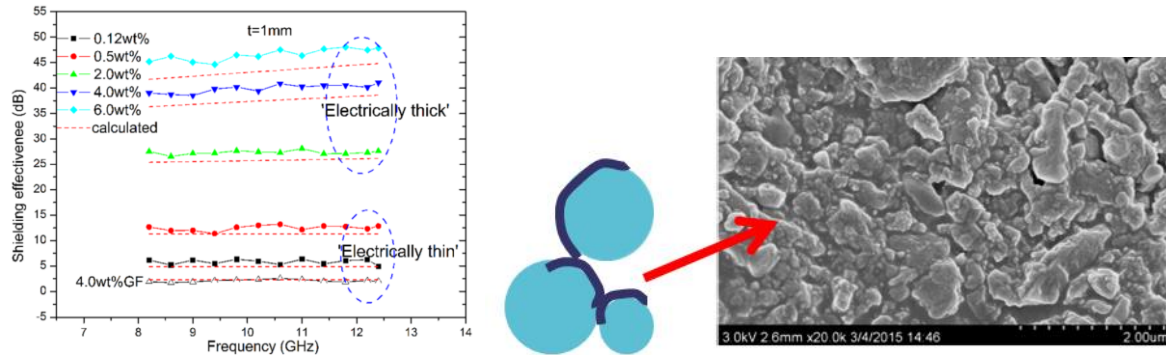


**Fig.18: Left: SE variations of GS/PA and GF/PA composites with different filler loadings at  $t=1$  mm (numbers in% indicate mass fraction of GS). Right : overview of composite and sketch showing a graphene flake wrapped around a PA ball <sup>xlix</sup>.**

The spherical latex particles help in the building 3D interconnected structures of the graphene agglomerated at their surface (very conductive 3D network). This also because the latex spheres helps to keep highly conductive mono-layer of graphene. Indeed thanks to graphene sheets we can increase the conductivity of the materials but also the absorption considering that graphene sheets, as pointed out by Li et al<sup>xliv</sup>., have high aspect ratio, larges interfaces, and high dielectric loss. Our approach in this field will be to be more deterministic in fabricating this kind of architectures (see fig.19) on large surface with potential implementation for roll-to-roll fabrication.

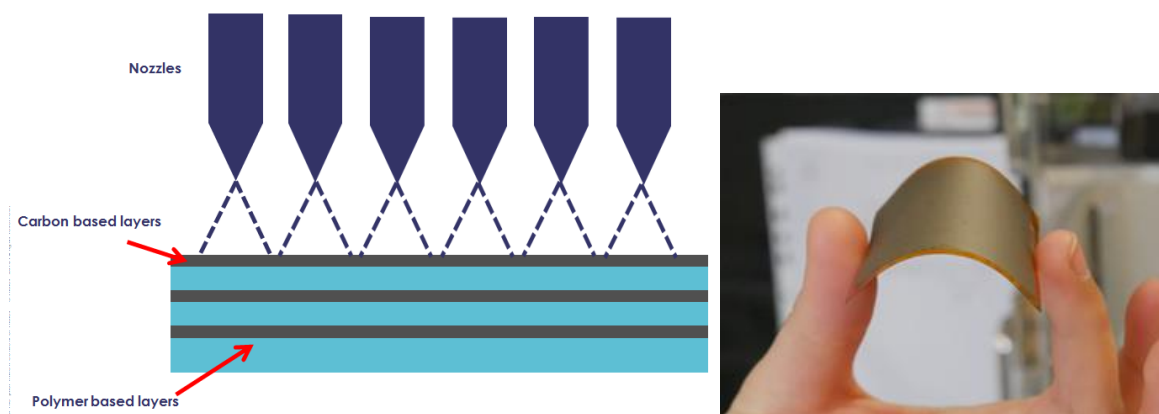


**Fig. 19: Left: Scheme of the approach to fabricate multi-layered structure for EMI applications using spray-gun deposition method. Thanks to the different layers we can enhance the Maxwell-Wagner-Sillars effect (and so the absorption to specific frequencies) but also the reflection enhancing the conductivity of the first layer creating a smart architecture. Right: first sample fabricated on kapton using polymers and graphene.**

Thanks to the new facility developed in the frame of the Graphene Flagship (see next paragraph for more details), we will be able to fabricate multi-layered structures. In this way we will be able to achieve, after design and modelling, structures with specific thickness and layers properties to tailor ad-hoc absorption at specific frequencies, with the possibility of raising also the conductivity and the reflection using graphene based layers to achieve smart structures. This could be a real breakthrough for this field and open new horizons of innovation.

### **Conclusions and new developments: from small to larger surfaces**

In this contribution we have highlighted the versatility and the large panel of applications of the dynamic spray-gun deposition especially for graphene related nanomaterials. This technique allows exploiting the potential of these materials and to fabricate devices that can impact our everyday life. The most impressive fact is that thanks to this fabrication method

we are able to achieve a nano-structuration of the materials deposited using a macro-technique of fabrication industrially suitable and potentially low-cost. This is an important breakthrough in the fabrication techniques field that can also be implemented for a large panel of applications with very large markets (see fig.20).

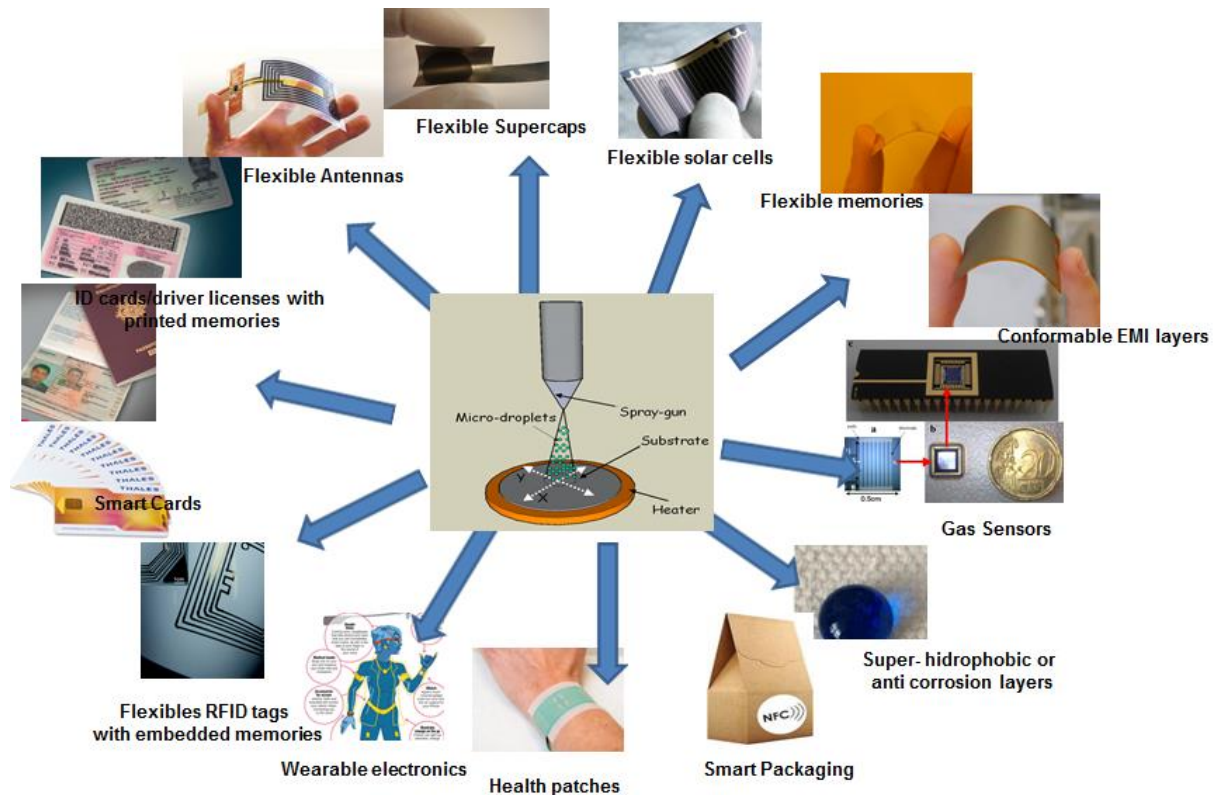


**Fig.20: Some of the potential applications that can be implemented using dynamic spray-gun deposition technique.**

Recently, in the frame of the Graphene Flagship project in 2018 we have developed, in collaboration with M-SOLV, a new machine able to fabricate larger samples that can allow the scale-up of the fabrication technique to strike large market (see fig.20). This machine is composed by four nozzles able to spray on a 30cmx30cm surface. This is the first and unique prototype of a new generation of machines that can be used in the future for a very large panel of applications changing the way in which the nanomaterials are effectively implemented in industrial applications. This is the result of more than ten years of

technological development that allows us moving from manual small surface machine to completely automatic large surface compatible facility (see fig.21).

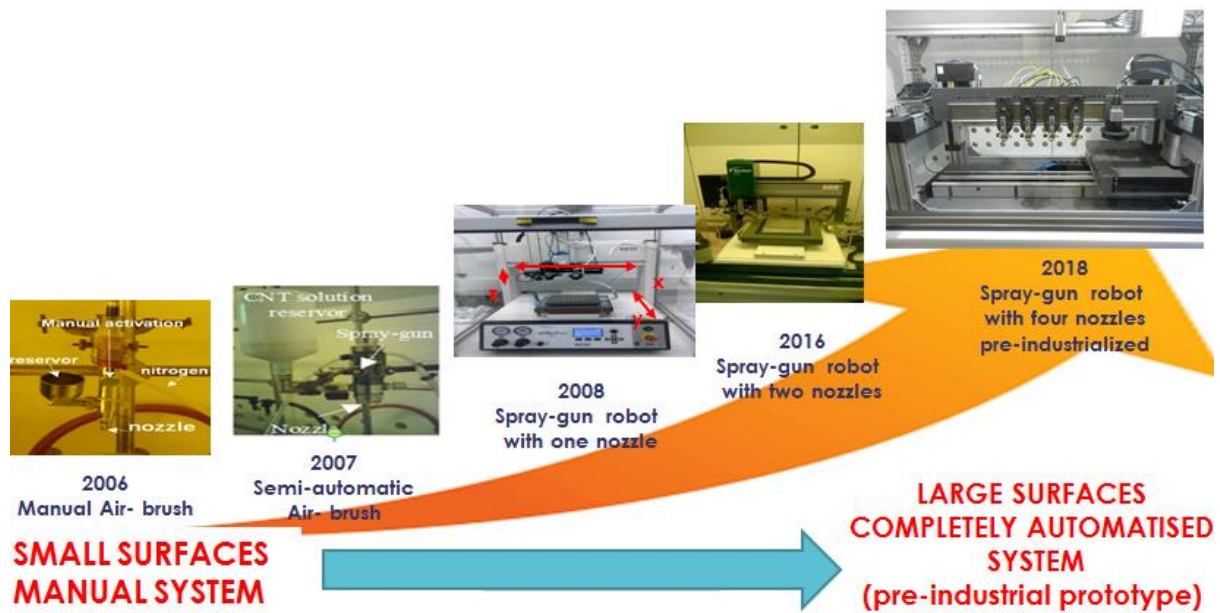


**Fig.21: History of the development of the dynamic spray-gun deposition method and of its implementation during the last ten years. In the right the four nozzles spray-gun deposition set-up (funded by Graphene Flagship project).**

Thanks to this machine we can imagine to spray layers of different nanomaterials and therefore to achieve the “lego view” for utilization of 2D materials suggested by Nobel Prize Andrew Geim in 2013<sup>1</sup> in a more realistic way without complex processes for the precise positioning of several single layers of 2D materials that is not suitable from industrial point of view also considering that the final cost of the devices strongly depends on the capacity to scale-up the process and to reduce the fabrication time. In this optics in the Graphene Flagship consortium, the conception and set-up of a roll-to-roll machine to fabricate supercapacitors by spray is in progress and will be ultimate during the next year (2019). This will constitute a completely new way of producing supercapacitors that could be widened in

1  
2  
3 the future for other applications already mentioned (see fig.21) exploiting different kind of  
4  
5 nanomaterials structuration on different kinds of substrates (e.g. paper, plastics).  
6  
7

## 8 **Acknowledgments**

9  
10  
11 This work was partially supported by the EU H2020 Projects “Modified Cost-Effective Fibre  
12  
13 Based Structures with Improved Multi-Functionality and Performance” (MODCOMP) under  
14  
15 Grant Agreement no. 685844, “Smart by Design and Intelligent by Architecture for turbine  
16  
17 blade fan and structural components systems” (SMARTFAN) under Grant Agreement no.  
18  
19 760779 and Graphene Flagship (FET flagship initiative Ramp-phase, Core 1, Core 2).  
20  
21  
22

23  
24 We would like to thanks Vincent Derycke of LICSEN (CEA Paris-Saclay/IRAMIS/NIMBE  
25  
26 UMR 3685), Adrian Balan (ex Post-doc at Thales/CEA), Gaetan Bracciale (LCMM/Thales  
27  
28 Research and Technology), Gregory Pognon (LCMM/ Thales Research and Technology),  
29  
30 Christophe Galindo (LCMM/ Thales Research and Technology), Gilles Feugnet  
31  
32 (LMN/Thales Research and Technology), Louis Gorintin (ex PhD Thales), Colin Delfaure  
33  
34 (ex Post-Doc Thales) for their contribution to the results shown in this work. A special  
35  
36 thanks for Francesco Bonaccorso, Vittorio Pellegrini, Alberto Ansaldo, Sebastiano Bellani,  
37  
38 Mirko Prato, Antonio Del Rio Castillo of the IIT Graphene Lab for the high quality graphene  
39  
40 provided in the frame of the Graphene Flagship project and strong collaboration in the frame  
41  
42 of the Graphene Flagship.  
43  
44  
45  
46  
47  
48  
49  
50  
51  
52  
53  
54  
55  
56  
57  
58  
59  
60

## References

- 
- i Kong J, Franklin N R, Zhou C, Chapline M G, Peng S, Cho K, Dai H, 2000 *Science* **287** (5453) 622-625
- ii Bondavalli P, Legagneux P, Pribat D, 2009 *Sens. Actuators B* **140** (1) 304–318.
- iii Bondavalli P, Gorintin L., Feugnet G., Lehouc G., Pribat D., 2014 *Sensors and Actuators B: Chemical* **202** 1290–1297
- iv CNTs for gas sensing, in: P. Bondavalli, L. Gorintin, P. Legagneux (Eds.), *Applications of Carbon Nanotubes*, Pan Stanford, 2011, ISBN: 9789814303187.
- v Peng N, Zhang Q, Chow C L, Tan O K, Marzari N, 2009 *Nano Lett.* **9** (4) 1626–1630.
- vi Zhang J, Boyd A, Tselev A, Paranjape M, Barbara P, 2006 *Appl.Phys.Lett.* **88**, 123112
- vii Heinze S, Tersoff J, Martel R, Derycke V, Appenzeller J, Avouris Ph., 2002 *Phys.Rev.Lett.* **89** (10) 106801
- viii Heinze S, Tersoff J, and Avouris P, 2003 *Appl. Phys. Lett.*, **83** (24) 5038–5040
- ix Derycke V, Martel R, Appenzeller J, Avouris Ph., 2002 *Appl.Phys.Lett.* **80** (15) 2773
- x Leonard F, Tersoff J, 2000 *Phys.Rev Lett.* **84** (20) 4693
- xi Cui X, Freitag M, Martel R, Brus L, Avouris Ph, 2003 *Nanolett.* **3** (6) 783-787, 2003
- xii Kumar S, 2006 *Applied Physics Letters* **89** 143501
- xiii Kumar S, Murthy J.Y., Alam M.A. 2005 *Physical Letters Review* **95** 066802
- xiv Fuhrer M S, Nygård J, Shih L, Forero M, Yoon Y-G, Mazzone M S C, Choi H-J., Ihm J, Louie SG , Zettl A, McEuen P L, 2000 *Science* **288** 494-497
- xv Hasan T, Scardaci V, Tan P H, Rozhin A G, Milne WI, Ferrari A C, 2007 *J. Phys. Chem.C* **111** (34) 12594–12602.
- xvi Coleman J N, 2009 *Advanced Functional Materials* **19** (23) 3680 3695

<sup>xvii</sup> Deegan R D, Bakajin O, Dupont T F, Huber G, Nagel S R, Witten T A, 2000 *Phys. Rev. E* **62** 756.

<sup>xviii</sup> Deegan R D, 2000 *Phys. Rev. E* **61** 475.

<sup>xix</sup> WO2012049428, Method for depositing nanoparticles on a surface and corresponding nanoparticle depositing appliance, Paolo Bondavalli, Pierre Legagneux, Louis Gorintin, 2012

<sup>xx</sup> WO2016124756 - Method of depositing oxidized carbon-based micro-particles and nanoparticles, Paolo Bondavalli, Gregory Pognon, Christophe Galindo, 2016

<sup>xxi</sup> Pribat D, Cojocar C S, Gowtham M, Eude L, Bondavalli P, Legagneux P, 2007 *Journal of the Society for Information Display* **15** (8) 595-600

<sup>xxii</sup> WO2006128828- Conductive nanotube of nanowire FET transistor network and corresponding electronic device, for detecting analytes, Paolo Bondavalli, Pierre Legagneux, Pierre Lebarney, Didier Pribat, Julien Nagle, 2006

<sup>xxiii</sup> Kaempgen M, Chan C K, Ma J, Cui Y, Gruner G, 2009 *Nano Lett.* **9**(5) 1872-6

<sup>xxiv</sup> Cheng Q, Tang J, Ma J, Zhang H, Shinyaa N, Qin L-C, 2011 *Phys. Chem. Chem. Phys.* **13** 17615

<sup>xxv</sup> Bondavalli P., Delfaure C., Legagneux P., Pribat D. 2013 *JECS* **160** (4) A1-A6

<sup>xxvi</sup> Ansaldo A, Bondavalli P, Bellani S, Del Rio Castillo A E, Prato M, Pellegrini V, Pognon G, Bonaccorso F, 2017 *ChemNanoMat.* **3** (6)436–446

<sup>xxvii</sup> Bondavalli P, Pognon G, Koumoulos E, Charitidis C 2018 *MRS Advances* <https://doi.org/10.1557/adv.2018.65>,

<sup>xxviii</sup> Bondavalli P *Graphene and Related Nanomaterials 1st Edition, Properties and Applications*, , Hardcover ISBN: 9780323481014, Elsevier, Published Date: 1st September 2017, 192p

<sup>xxix</sup> <http://www.itrs2.net/2011-itrs.html>

1  
2  
3  
4 xxx Bondavalli P, Ihnatov D, Pribat D, Legagneux P Chapter 18. *Resistive Nonvolatile*  
5  
6 *Memories Based on Graphene-Related Materials: State of the Art in Graphene Science*  
7  
8 *Handbook, Applications and Industrialization*, Edited by Mahmood Aliofkhaeaei, Nasar Ali,  
9  
10 William I. Milne, Cengiz S. Ozkan, Stanislaw Mitura, and Juana L. Gervasoni CRC Press  
11  
12 2016, pp 269–278

13  
14  
15 xxxi Bondavalli P Chapter 9., *Graphene oxides ReRAM in Rad-Hard semiconducting*  
16  
17 *memories*, River Publishers Series in Electronic Materials and Device, Cristiano Calligari and  
18  
19 Umberto Gatti, Ed Rivers Publishers 2019 to be published

20  
21  
22 xxxiii Wang C, Wu H, Gao B, Zhang T, Yang Y, Qian H, 2018 *Microelectronic Engineering*  
23  
24 **187–188** 121-133

25  
26  
27 xxxiii Chang T-C, Chang K-C, Tsai T-M, Chu T-J, Sze S M, *Materials Today* **19** (5) 254-264

28  
29  
30 xxxiv Waser R, Masakazu A 2007 *Nature Materials* **6** (11) 833–840.

31  
32  
33 xxxv Jeong H Y , Yun Kim O, Won Kim J, Hwang J O, Kim J-E, Yong Lee J, Yoon T H, Cho  
34  
35 B J, Kim SO, Ruoff R S, Choi S-Y, 2010 *Nanolett.* **10** 4381-4386

36  
37 xxxvi He C L, Zhuge F, Zhou X F, Li M, Zhou G C 2009 *Appl. Phys. Lett.* **95** 232101

38  
39  
40 xxxvii Dikin D A, Stankovich S, Zimney E J, Piner R D, Dommett G H B, Evmenenko G,  
41  
42 Nguyen S T, Ruoff R S 2007 *Nature* **448**, 457–460

43  
44 xxxviii Hong S K, Kim J E, Kim S O, Cho B J, 2010 *J of Appl. Phys.* **31** 1005

45  
46 xxxix <http://modcomp-project.eu/>

47  
48 xl Agraït N, Levy Yeyati A, Van Ruitenbeek J M, 2003 *Physics Reports* **377** 2–3 81-279

49  
50 xli Geetha S, Kumar K K S, Rao C R K, Vijayan M, Trivedi 2009 D C J.of Appl. Polymer  
51  
52 Science **112** (4)

53  
54 xlii Wen B et al 2014 *Adv. Mater.* **26** 3484

55  
56  
57 xliii Zhang Y et al 2015 *Adv. Mater.* **27** 2049.  
58  
59  
60

1  
2  
3  
4 xlv Li N, Huang Y, Du F, He X, Lin X, Gao H, Ma Y, Li F, Chen Y, Eklund P C 2006 *Nano*  
5  
6 *Lett.* **6** (6) 1141-1145

7  
8  
9 xlv Advanced Materials for Electromagnetic Shielding: Fundamentals, Properties, and  
10 Applications, Maciej Jaroszewski (Editor), Sabu Thomas (Editor), Ajay V. Rane (Editor)  
11  
12 ISBN: 978-1-119-12861-8 2018 464

13  
14  
15  
16 xlvii McKenzie R, Zurawsky W, Mijovic J 2014 *Journal of Non-Crystalline Solids* **406** 11-21

17  
18  
19 xlviii Xia X, Zhong Z, Weng G J, 2017 *Mechanics of Materials* **109** 42-50

20  
21  
22 xlix Xia X, Wang Y, Zhong Z, Weng G J., 2017 *Carbon* **111** 221-230

23  
24  
25  
26  
27  
28  
29  
30  
31  
32  
33  
34  
35  
36  
37  
38  
39  
40  
41  
42  
43  
44  
45  
46  
47  
48  
49  
50  
51  
52  
53  
54  
55  
56  
57  
58  
59  
60  
xlix Li Y, Zhang S, Ni Y, 2016 *Mater. Res. Express* **3** 075012

l Geim A K, Grigorieva I V, 2013 *Nature* **499** 419–425